Comparative proteomics analysis of the responses to cigarette smoke particulate matter in six plant species leaves

Bayu Hadi Permana
King Mongkut's University of Technology Thonburi
Phitthaya Nookongbut
King Mongkut's University of Technology Thonburi
Sucheewin Krobthong
Kasetsart University
Yodying Yingchutrakul
National Omics Center, NSTDA, Pathum Thani
Treenut Saithong
King Mongkut's University of Technology Thonburi
Paitip Thiravetyan
King Mongkut's University of Technology Thonburi
Chairat Treesubsuntorn
chairat.tre@kmutt.ac.th

King Mongkut's University of Technology Thonburi

Research Article

Keywords: Cigarette smoke, Particulate matter, Plant-PM response, Plant proteomics, Photosynthesis

Posted Date: June 22nd, 2023

DOI: https://doi.org/10.21203/rs.3.rs-3065688/v1

Additional Declarations: No competing interests reported.

Abstract

Phytoremediation has been recognized to reduce particulate matter (PM) concentration in the air. Plant stress response plays a crucial role in PM removal. In this study, six plants including ornamental and perennial plants were exposed to PM from cigarette smoke for 24 hours. Ornamental plants were *Calathea makoyana*, *Sansevieria trifasciata*, and *Zamioculcas zamiifolia*, where perennial plants *Bauhina purpurea*, *Tectona grandi*, and *Wrightia religiosa*. The initial concentration of PM was 300–320, 400–450, and 500–530 μg m^{-3} for $PM_{1.0}$, $PM_{2.5,}$ and PM_{10}, respectively. The plant response of each plant was compared to determine the plant response of each group and plant against PM stress. The results showed that all plants have different protein expressions. Ornamental plants showed more enrichment in photosynthesis and antioxidant enzymes, whereas perennial plants were in photosynthesis, an antioxidant enzyme, and carbon metabolism. The results suggest the plant response of each plant of an ornamental and perennial plant. This proteomics approach was useful for future studies, especially for phytoremediation.

1. Introduction

Particulate Matter (PM), a primary air pollutant that has become one of the most critical air pollutants worldwide. Today, almost all of the world's population is living in places with poor air quality leading the World Health Organization (WHO) to consider air pollution as the biggest environmental health human problem (Liang et al., 2016). Man-made sources contributing, vehicle exhaust, cement factories, and industrial processors emit mainly PM directly (Urrutia-Mosquera and Flórez-Calderón, 2023). Secondary particle reactions generate secondary PM in the atmosphere by the reaction of other toxic pollutants such as nitrogen oxides (NOx), sulfur dioxide (SO_2), ammonia, and volatile organic compounds (VOCs) (Tajuelo et al. 2021). There are several deleterious PM effects, often forming a complex mixture with highly toxic components, such as carcinogens. Kim et al. (2021) remarked PM in the atmosphere responds to a high risk of adverse harmful effects to human health, chronic obstructive pulmonary diseases (COPD) such as lung cancer and cardiopulmonary disease. People living in the fastest growing cities in the world are exposed to pollution levels that are exceeded many times over. The WHO air quality guidelines stated the mean limits for exposure to PM. This will cause great trouble in the future in terms of public health with massive medical and social costs. For this reason, there is an emergency response to address growing environmental problems and implement abatement related to air pollution (Jin et al., 2021). PM pollution in cities is more likely to develop in winter from human activities such as industrial facilities, and fossil fuel vehicles as well as in summer may also intensity PM concentrations due to open burning of agricultural residues and forest fires for preparation of cropping areas (Tiyapairat, 2012). Moreover, summer can increase secondary PM (Wang et al., 2016). Therefore, it is an emergency to prepare to develop technology to cope with PM concentrations.

Phytoremediation has been recognized as one of the most scientific technologies that have been made to reduce PM for the well beings of humans, animals as well as plants (Paull et al., 2019; Popek et al., 2015). Plant species play a significant role in the effect on its capability of reducing speed velocity and

capturing PM (Nakazato et al., 2018) and complement air pollution mitigation by vegetated greenbelts (Wang, 2011). As PM exposures on the aerial surfaces of plants, it has been exhibited to reduce photosynthetic efficiency, affect physiological plant disorders, and increase the wax layer (Treesubsuntorn et al., 2021). Leaf area directly affected accumulation, while petiole length and internodal distance had opposite effects. The experimental site had significantly higher average particulate deposits compared to the control site. 80.95% of species accumulated more particles in the experimental site, while only 19.04% did so in the control site. Both parameters showed distinct seasonal patterns. *Butea monosperma*, *Tectona grandis*, and *Diospyros melanoxylon* had high particle capture capacities with efficiency rates of 48.44%, 41.71%, and 32.09% respectively (Sahu et al.. 2021). However, PM stresses have distinguished effects on plant growth and the metabolic process (Rai, 2016). To combat such stresses, plants have evolved complex but not well-understood responses. Thus, for knowledge-based proving strategies for PM-tolerant plants, an understanding of the molecular PM-tolerance mechanisms of plants is more required. This study used six plants, such as perennial trees (including *Bauhinia purpurea*, *Tectona grandi*, and *Wrightia religiosa*) and ornamental plants (including *Calathea makoyana* E.Morren, *Sansevieria trifasciata* Prain, and *Zamioculcas zamiifolia* (Lodd.) Engl). The plants have reported good efficiency to remove $PM_{2.5}$ and other VOCs in previous studies (Siswanto et al., 2020; Sriprapat et al., 2014; Sriprapat & Thiravetyan, 2016; Treesubsuntorn et al., 2021). The plants that are exposed to PM depend on phenotypic plasticity for remodeling during developmental or facilitating survival under stressful environmental conditions changes (Swindell et al., 2007). Proteomics is a high-throughput tool for investigating obtains qualitative and quantitative analyses of experimental conditions of different biochemical pathways including plant stress-related responses (Shen et al., 2021; Hong et al., 2020). Moreover, proteomics also serves as a vital tool in bridging the gap between transcriptomics and metabolomics as it facilitates genomic studies. In particular, comparative proteomic analysis of plant species exposed to PM stress conditions allows for the investigation of various response-related mechanisms adopted by plants grown under these stress conditions (Cook et al., 2004). Within the past few years, LC-MS/MS has become the method of choice for obtaining an insight into the biochemical and proteome maps of plants (Rashid et al., 2013). Furthermore, differential proteomics profiles could contribute to the identification and characterization of PM stress-responsive proteins that could be used as biological markers for the study of a PM stress response.

In the previous work, plant species exhibited good PM and VOC remediation (Treesubsuntorn et al., 2021). However, under highly concentrated stress exceeds, the plant has been demonstrated a reduction in efficiency, and plant physiology is still unclear. In the present study, to further explore the plant-mediated mechanism of PM response, which performed a proteomic level analysis of the raw proteomic data again. To investigate the Plant-PM interaction, we conducted a proteomic analysis on perennial trees and ornamental plants. The objectives of this research were to: (1) identify proteins expressed in protein profile changed response to PM exposure in ornamental and perennial plants; (2) analyze the mechanism undergone under PM stress in ornamental and perennial plants. The knowledge gained from this study will be instrumental in understanding the molecular mechanisms involved in the response to PM exposure.

2. Materials and methods

2.1 Plant material and sample collection

This research is a study of the PM affect induced proteome changes in plant leaves related to plant materials were collected from 3 perennial trees (including *Bauhinia purpurea*, *Tectona grandi*, and *Wrightia religiosa*) and 3 ornamental plants (including *Calathea makoyana* E.Morren, *Sansevieria trifasciata* Prain and *Zamioculcas zamiifolia* (Lodd.) Engl). All six plant species were selected based on the good air pollutant removal from our previous reports at the Remediation Laboratory, King Mongkut's University of Technology Thonburi (KMUTT), Bangkok, Thailand. All species are common plants in Thailand and are widely grown in urban areas. For each species, three similar individuals were used as replicates for the experiment. Condition to grow plants before experimental initiation, all six plant species were cultivated under natural environmental conditions at Remediation Laboratory, KMUTT, Bangkok, Thailand. The trees were grown in loam soil supplemented by coconut coir which was purchased from plant shops in Bangkok, Thailand. Plants were watered every other day with optimal tap water and watered plants daily. Healthy and no sign of diseases plants were used for further experiment. The responses of plant species growing in the PM exposure have generally been investigated in terms of protein profiles obtained from potted plants.

2.2 PM exposure

The leaves of the test plant species were pretreated by washing with tap water and naturally dried, and the pots were wrapped with aluminum foil. Each potted plant was placed inside the cleaned 1 m^3 testing chamber. Particulate matter was produced from cigarette smoke, Experiments were conducted by using a vacuum pump to suck the smoke from the gas preparation chamber into the testing chamber. In addition, plants without PM exposure served as control plants. PM was generated from cigarette smoke. Experiments were carried out by using a vacuum pump to suck the smoke from the gas preparation chamber and injected it into the testing chamber. The initial PM concentrations were 300–320, 400–450, and 500–530 μg m^{-3} for $PM_{1.0}$, $PM_{2.5,}$ and PM_{10}, respectively. The experiments were carried out in triplicate under fluorescent light with a ~ 16 h photoperiod. Plants were maintained in a growth chamber at 28 ± 3°C and 70% relative humidity under a 16:8 h photoperiod (day/night) for 24 h. the plant treatment and control were harvested. To establish the proteomic analyses samples, plant leaves material of approximately 500 mg was collected and frozen in liquid nitrogen. The samples were then ground using a mortar and either stored at -80°C for further protein extraction.

2.3 Proteomics sample preparation for proteomic analysis

To identify proteins involved in PM exposure, an optimized protein extraction method for gel-free proteomic analysis was presented in this work. The total proteins were extracted for each of the three biological replicates according to the Niu et al. method (2018). Briefly, the leaf powder was extracted by resuspended fresh hypotonic cell lysis buffer (0.2% SDS, 20 mM DTT, 10 mM HEPES-KOH, pH 8.0 (1:5 w/v ratio)). The cell lysis solution was precipitated by 15% TCA/acetone precipitation at a 20:80 (v/v)

ratio and washed with cold acetone (twice). After precipitation, the protein pellet was reconstituted in 0.25% RapidGest SF (Waters, UK) in 10 mM Ammonium bicarbonate (fresh prepared) to improve in-solution protein digestion in terms of speed and peptide recovery. The Lowry assay (BSA as protein standard) method was used to estimate total protein concentration. Next, the proteins 25 µg of protein was subjected to gel-free based digestion. The reduction and alkylation of proteins were performed by using 5 mM DTT and incubated at 80°C for 20 minutes and then alkylation of sulfhydryl groups by using 25 mM IAA was carried out at room temperature for 30 minutes in the dark. The solution was purified by a 7 kDa molecular weight cut-off, 0.5 mL (Zeba™ Spin Desalting Columns, ThermoFisher, USA). Proteolytic cleavage of digestive enzymes process by using 500 ng of sequencing grade trypsin (Promega, Germany) was added to the protein solution and incubated at 37°C for 3 hours. The peptides were redissolved in 0.1% formic acid/LC-MS water and transferred to a TruView LCMS vial (Waters, UK).

2.4 LC-MS/MS and data processing

The peptide mixture samples were analyzed in tandem mass spectrometers (Orbitrap HF hybrid mass spectrometer combined with an UltiMate 3000 LC system) (Klein et al., 2016). Briefly, Peptides were separated in reverse phase mode online using a C18 PepMap 100 trapping column, before being resolved onto a C18 PepMap™ 100 capillary column with a 70-min gradient of acetonitrile, 0.1% formic acid, at a flow rate of 300 nL/min. Peptides were analyzed by implementing a data-dependent standard top 15 method including a scan cycle initiated by a full scan of peptide ions in the Orbitrap analyzer, accompanied by high-energy collisional dissociation and MS/MS scans on the 15 most abundant precursor ions. Full scan mass spectra were acquired from *m/z* 400 to 1600 with an automatic gain control (AGC) target set at 3×10^6 ions and a resolution of 60,000. MS/MS scan was initiated when the ACG target reached 10^5 ions with a threshold intensity of 83,000 and potential charge states of 2^+ and 3^+. Ion selection was accomplished by applying a dynamic exclusion window of 12 seconds (Trapp et al., 2016).

2.5 Analysis of the differential abundance of proteins acquired using mass spectrometry

All raw files were analyzed by the Proteome Discoverer software version for initial analysis. 2.4 (PD) (Thermo Scientific) using the SEQUEST, Percolator, and Minora algorithms.

LC-MS spectrum protein database matches, and finally, non-redundant protein groups using the principle of strict parsimony as defined by the UniProtKB reviewed database (11/01/2020). For protein identification and quantification, the setting parameters were as follows: The following parameters were applied for MS/MS spectra assignment: full-trypsin specificity, a maximum of two trypsin missed cleavages were allowed with a precursor mass tolerance of 5 ppm on the parent ion and fragment mass tolerance of 0.01 Da. A fixed modification, Carbamidomethylation Cysteine + 57.021 Da. and oxidized Methionine + 15.995 Da. were selected as dynamic modifications. The False discovery rate (FDR) of peptide and protein identification were both set to 0.05. The normalization of the relative protein abundances ratio was operated by total peptide amount for each LC-runs (across all runs; n = 6) by the

normalization algorithm of Proteome discoverer software. To assemble a differentially expressed protein list, multiple consensus workflows were used to determine the differential protein expression of the samples. The proteins identified data have been deposited to the ProteomeXchange Consortium via the PRIDE partner repository with the dataset identifier PXDxxxx (Vizcaino et al., 2013). Differential expression proteins were determined by criteria, such as protein only found in all replicates (n = 3), p-value < 0.05, and the abundance ratio of treatment per control for upregulated and downregulated were above 1.5 and below 0.5, respectively. Proteins were categorized based on function using Hierarchical clustering analysis and Gene Ontology (GO) analysis which are affected by PM stress. The functionally annotated proteins from PM exposed and unexposed samples were categorized into GO terms (molecular function, cellular function, biological function, and protein class) was performed with the set of all protein-coding genes in the *Arabidopsis* genome, the pathway enrichment analysis was done using Kyoto Encyclopedia of Genes and Genomes (KEGG) by using accession number as an ID (Raudvere et al., 2019).

3. Results and discussion

3.1 Different responses of ornamental and perennial plants under PM stress

Plant such as ornamental and perennial plants are exposed to PM with concentrations of 300–320, 400–450, and 500–530 μg m^{-3} for $PM_{1.0}$, $PM_{2.5,}$ and PM_{10}, respectively. After 24 hours of exposure, the leaf samples of each plant were taken and determine the proteins. The result showed that ornamental and perennial plants have different responses against PM (Fig. 1). Some plants' proteins disappeared due to static and criteria. Some ornamental plants tend more sensitive than perennial plants and are most active in the photosynthesis process whereas some perennial plants are tended to mostly in carbon metabolism. Based on the results, proteins in chloroplasts were more crucial and responsive than other organelles.

3.2 Photosynthesis mechanism of ornamental and perennial plants under PM stress

Both ornamental and perennial plants were exposed to PM stress from cigarette smoke. However, both types of plants showed different expressions of photosynthetic proteins. Most plants showed an increased abundance of oxygen-evolving complex proteins

(Tables 1 and 2). The protein was a key for redox catalyst and splitting of water when photosynthesis occurs, located in the photosystem II complex (Gupta, 2020; Ifuku et al., 2010). The process generates dioxygen and hydrogens which these hydrogens contribute to ATP phosphorylation (Gupta, 2020; Paul et al., 2017). The results might also indicate both ornamental and perennial plants were more active in water usage under PM stress to generate ATP and organic compounds. As theorized, water is an

important factor in the plant process, especially in photosynthesis. The result might be consistent with a previous study that found high water content giving positively correlated with plant health under PM stress (Treesubsuntorn et al., 2021). Under PM conditions, photosystem I (PSI), II (PSII), and light-harvesting complex (LHC) of *C. makoyana* showed downregulated. In contrast, *Sansevieria trifasciata* uniquely expressed PSII and LHC under stress conditions. *Zamioculcas zamiifolia* is mostly enriched in PSI, LHCI, and photosynthetic electron transport. The results might indicate that *C. makoyana* was more sensitive to PM stress, while *S. trifasciata* and *Z. zamiifolia* might able to manage the stress and maintain photosynthesis by increasing either one of the photosystem complex proteins. Similar to *S. trifasciata*, *B. purpurea* and *W. religiosa* were enriched in PSII-related proteins, while *Tectona grandi* was not shown enriched in photosynthesis. Both *W. religiosa* and *B. purpurea* enriched in the LHC part of PSII, ATP synthase, and carbon fixation. Therefore, *S. trifasciata*, *Z. zamiifolia*, *B. purpurea*, and *W. religiosa* might maintain and be more active in photosynthetic proteins under PM stress plants, while *C. makoyana* and *T. grandi* might not focus on this reaction.

Table 1
Photosynthetic proteins of ornamental plants under 24 h PM stress. Initial PM concentrations were 300–320, 400–450 and 500–530 μg m^{-3} for $PM_{1.0}$, $PM_{2.5}$ and PM_{10}, respectively.

Accession number	Protein name	Log2 fold change (T/C)
Calathea makoyana		
O62964	Ribulose bisphosphate carboxylase large chain	2.00
O65107	Photosystem I reaction center subunit N, chloroplastic	2.00
P93906	Ribulose bisphosphate carboxylase large chain	0.68
P05310	Photosystem I P700 chlorophyll a apoprotein A1	0.31
P26320	Oxygen-evolving enhancer protein 1, chloroplastic	0.28
Q9SAU2	Ribulose-5-phosphate-3-epimerase, chloroplastic	0.26
P59702	Cytochrome b559 subunit alpha	-0.31
P12359	Oxygen-evolving enhancer protein 1, chloroplastic	-0.33
P27522	Chlorophyll a-b binding protein 8, chloroplastic	-0.34
A6YGB8	Photosystem II protein D1	-0.62
Q9SUI5	Photosystem I reaction center subunit psaK, chloroplastic	-1.01
Q9SHE8	Photosystem I reaction center subunit III, chloroplastic	-2.00
P41758	Phosphoglycerate kinase, chloroplastic	-2.00
Q9XF89	Chlorophyll a-b binding protein CP26, chloroplastic	-2.00
Sansevieria trifasciata		
P12302	Oxygen-evolving enhancer protein 2, chloroplastic	Unique
P20866	Chlorophyll a-b binding protein, chloroplastic	Unique
P06260	NAD	Unique
Q9M3C6	Photosystem I assembly factor PSA3, chloroplastic	Unique
P48187	Photosystem II CP43 reaction center protein	Unique
Q8M9W4	Photosystem II D2 protein	Unique
P17067	Carbonic anhydrase, chloroplastic	Unique
Zamioculcas zamiifolia		
A6H5G7	Photosystem II CP43 reaction center protein	0.85

Accession number	Protein name	Log2 fold change (T/C)
Q42029	Oxygen-evolving enhancer protein 2 – 1, chloroplastic	0.69
Q32RX2	Cytochrome f	0.63
P27522	Chlorophyll a-b binding protein 8, chloroplastic	0.55
A9L9A4	Ribulose bisphosphate carboxylase large chain	0.53
Q39654	Photosystem I reaction center subunit XI, chloroplastic	0.46
P27491	Chlorophyll a-b binding protein 7, chloroplastic	0.35
P08221	Chlorophyll a-b binding protein of LHCII type I, chloroplastic	0.32
P12355	Photosystem I reaction center subunit III, chloroplastic	0.32
P09755	Chlorophyll a-b binding protein 2, chloroplastic	0.32
P10708	Chlorophyll a-b binding protein 7, chloroplastic	0.30
P23322	Oxygen-evolving enhancer protein 1, chloroplastic	0.29
Q40407	Oxygen-evolving enhancer protein 2, chloroplastic	0.27
Q9M158	Rhodanese-like domain-containing protein 4, chloroplastic	0.27
O20250	Transketolase, chloroplastic	0.24
Q6ZFJ3	Ferredoxin–NADP reductase, leaf isozyme 2, chloroplastic	0.24
P49107	Photosystem I reaction center subunit N, chloroplastic	0.19
P12360	Chlorophyll a-b binding protein 6A, chloroplastic	0.18
P22179	Photosystem I reaction center subunit VI, chloroplastic	-0.31
Q5Z5A8	Photosystem II stability/assembly factor HCF136, chloroplastic	-0.32
Q9BBQ5	Cytochrome b6-f complex subunit 4	-0.32
P54773	Photosystem II 22 kDa protein, chloroplastic	-0.38
P81372	Ferredoxin-A	-0.60
Q9BBQ7	Photosystem II reaction center protein H	-0.64
P00221	Ferredoxin-1, chloroplastic	-0.90

Table 2
Photosynthetic proteins of perennial plants under 24 h PM stress. Initial PM concentrations were 300–320, 400–450 and 500–530 μg m^{-3} for $PM_{1.0}$, $PM_{2.5}$ and PM_{10}, respectively.

Accession number	Protein name	Log2 fold change (T/C)
Bauhinia purpurea		
Q9TL00	Photosystem II D2 protein	2.00
Q49CC1	Ribulose bisphosphate carboxylase large chain	0.85
P41758	Phosphoglycerate kinase, chloroplastic	0.51
P25856	Glyceraldehyde-3-phosphate dehydrogenase GAPA1, chloroplastic	0.49
O62964	Ribulose bisphosphate carboxylase large chain	0.36
P09044	Glyceraldehyde-3-phosphate dehydrogenase B, chloroplastic	0.36
P12468	Ribulose bisphosphate carboxylase small subunit, chloroplastic 2	0.33
Q07473	Chlorophyll a-b binding protein CP29.1, chloroplastic	0.31
P22418	Fructose-1,6-bisphosphatase, chloroplastic	0.29
Q42796	Fructose-1,6-bisphosphatase, chloroplastic	0.27
Q9SAU2	Ribulose-5-phosphate-3-epimerase, chloroplastic	0.27
P12113	ATP synthase gamma chain, chloroplastic	0.21
P27522	Chlorophyll a-b binding protein 8, chloroplastic	0.20
P31186	Ribulose bisphosphate carboxylase large chain	0.19
P08221	Chlorophyll a-b binding protein of LHCII type I, chloroplastic	0.18
Q49KW9	Photosystem II reaction center protein H	-0.38
Q06SI3	Ribulose bisphosphate carboxylase large chain	-0.82
Q9LD57	Phosphoglycerate kinase 1, chloroplastic	-2.00
Q06SH5	Photosystem II D2 protein	-2.00
Tectona grandi		
Q41932	Oxygen-evolving enhancer protein 3 – 2, chloroplastic	0.36
Q07473	Chlorophyll a-b binding protein CP29.1, chloroplastic	-0.45

Accession number	Protein name	Log2 fold change (T/C)
Q9SAU2	Ribulose-5-phosphate-3-epimerase, chloroplastic	-0.62
Wrightia religiosa		
Q06RA6	Photosystem II CP47 reaction center protein	Unique
P26320	Oxygen-evolving enhancer protein 1, chloroplastic	Unique
Q9BBQ5	Cytochrome b6-f complex subunit 4	Unique
Q42796	Fructose-1,6-bisphosphatase, chloroplastic	Unique
Q09G20	Photosystem II CP47 reaction center protein	Unique
Q49CC1	Ribulose bisphosphate carboxylase large chain	2.00
Q3BAK7	Cytochrome b6	0.78
O49079	Oxygen-evolving enhancer protein 1, chloroplastic	0.78
P27141	Carbonic anhydrase, chloroplastic	0.62
Q1ACK0	Ribulose bisphosphate carboxylase large chain	0.56
P43224	Ribulose bisphosphate carboxylase large chain	0.53
A0A364	Photosystem II reaction center protein H	0.48
Q9SHE8	Photosystem I reaction center subunit III, chloroplastic	0.48
A0A335	Photosystem I P700 chlorophyll a apoprotein A1	0.44
Q06RC1	Ribulose bisphosphate carboxylase large chain	0.41
P28407	Ribulose bisphosphate carboxylase large chain	0.41
A7M942	Photosystem I iron-sulfur center	0.40
P80471	Light-induced protein, chloroplastic	0.38
Q8S8X5	Photosystem I P700 chlorophyll a apoprotein A2	0.38
P85189	Oxygen-evolving enhancer protein 2, chloroplastic	0.38
P36494	Chlorophyll a-b binding protein CP24, chloroplastic	0.38
Q42961	Phosphoglycerate kinase, chloroplastic	0.34
P48693	Ribulose bisphosphate carboxylase large chain	0.32
P07371	Chlorophyll a-b binding protein AB80, chloroplastic	0.32
P25856	Glyceraldehyde-3-phosphate dehydrogenase GAPA1, chloroplastic	0.32

Accession number	Protein name	Log2 fold change (T/C)
Q42676	Transketolase, chloroplastic	0.31
Q9S841	Oxygen-evolving enhancer protein 1–2, chloroplastic	0.30
P49107	Photosystem I reaction center subunit N, chloroplastic	0.30
A9L9C2	Photosystem II CP47 reaction center protein	0.29
P48688	Ribulose bisphosphate carboxylase large chain	0.28
Q9SAU2	Ribulose-5-phosphate-3-epimerase, chloroplastic	0.28
P05435	ATP synthase gamma chain, chloroplastic	0.26
P25857	Glyceraldehyde-3-phosphate dehydrogenase GAPB, chloroplastic	0.25
A4GGA1	Photosystem II CP43 reaction center protein	0.25
P69568	Ribulose bisphosphate carboxylase large chain	0.24
A0A348	Cytochrome f	0.24
Q9XFT3	Oxygen-evolving enhancer protein 3 – 1, chloroplastic	0.23
P27494	Chlorophyll a-b binding protein 36, chloroplastic	0.22
A6YGB8	Photosystem II protein D1	0.22
Q06FL3	Cytochrome f	0.22
A6YG76	Photosystem II D2 protein	0.21
Q9SYW8	Photosystem I chlorophyll a/b-binding protein 2, chloroplastic	0.20
Q32701	Ribulose bisphosphate carboxylase large chain	0.20
P08221	Chlorophyll a-b binding protein of LHCII type I, chloroplastic	0.19
A6MM49	Cytochrome f	-0.33
Q10HD0	Chlorophyll a-b binding protein, chloroplastic	-0.41
P27522	Chlorophyll a-b binding protein 8, chloroplastic	-0.41
Q9SUI4	Photosystem I reaction center subunit XI, chloroplastic	-0.42
P46486	Photosystem I reaction center subunit III, chloroplastic	-0.44
P43229	Ribulose bisphosphate carboxylase large chain	-0.48

Accession number	Protein name	Log2 fold change (T/C)
Q8VXQ9	Glyceraldehyde-3-phosphate dehydrogenase A, chloroplastic	-0.51
P12353	Photosystem I reaction center subunit II, chloroplastic	-0.58
Q9S7N7	Photosystem I reaction center subunit V, chloroplastic	-0.69

3.3 Antioxidant protein involved in ornamental and perennial plants under PM exposure

Ornamental plants showed less expressed antioxidant proteins than perennial plants (Fig. 2). The antioxidant enzymes, peroxiredoxin (Q6ER94 and Q9SDD6) and superoxide dismutase (O65175) in *C. makoyana* were not expressed under PM exposure. In contrast, under PM exposure, *S. trifasciata* has upregulated peroxiredoxin and superoxide dismutase. Most of the antioxidant enzymes of *Z. zamiifolia* plant showed downregulated under PM exposure, only ascorbate peroxidase (Q05431) and catalase (P07145) were upregulated. Antioxidant enzymes play role in oxidative stress scavenging. Downregulated antioxidant enzymes will accumulate reactive oxygen species (ROS) that will damage the plant cells (Foyer, 2018). Different from ornamental plants, most perennial plants' antioxidant-related proteins showed upregulated. This showed that in general, perennial plants are more resilient than ornamental plants against PM stress from cigarette smoke. Plants like *S. trifasciata*, *B. purpurea*, and *W. religiosa* that enriched to photosynthesis process under PM exposure, showed upregulated specialized antioxidants in chloroplasts, such as superoxide dismutase, ascorbate peroxidase, and peroxiredoxin-type. The results might indicate that the plants tend to prevent oxidative damage from active photosynthesis under PM stress in the crucial site. As theorized in the previous studies that ROS can be generated in abundance by photosynthesis, therefore, the presence of antioxidants is necessary for chloroplasts (Foyer, 2018; Tripathy & Oelmüller, 2012; Xiong et al., 2021). In chloroplast, photosynthesis produces singlet oxygen at PSII, the superoxide is changed to hydrogen peroxide (H_2O_2) by superoxide dismutase, therefore, H_2O_2 is converted to water by ascorbate peroxidase and peroxiredoxin (Foyer, 2018).

3.4 Carbon fixation, pentose phosphate pathway and photorespiration in ornamental and perennial plants

Ornamental and perennial plants under PM stress are enriched in carbon metabolism. Based on the results, most protein-related in *C. makoyana* were downregulated (Fig. 3). Plant *W. religiosa* and *B. purpurea* became the most active carbon fixation mechanism (Fig. 3). Plant *Z. zamiifolia* and *W. religiosa* were enriched in the non-oxidative pentose phosphate pathway (PPP). Interestingly, two plants upregulated transketolase (AT2G45290) in the mechanism. The enzyme plays role in catalyzing the carbon-carbon bond in the keto sugars (Henderson & Toone, 1999). The pentose phosphate shunt is used to generate pentose phosphate for nucleic acid and amino acid formation (Henderson & Toone, 1999). Photorespiration was enriched by both ornamental and perennial plants, except *C. makoyana*.

Interestingly, the conversion of glycolate to glyoxylate generates H_2O_2, this lead to antioxidant enzymes specialized in peroxisome being upregulated (Fig. 2). Moreover, *Z. zamiifolia*, *B. purpurea*, and *T. grandi* might convert glycine to ammonia (NH_3), in contrast, *S. trifasciata* might convert glycine to serine, whereas *W. religiosa* might involve in both processes (Fig. 4). The results might assume that plants generated ammonia and used it for glutamate synthesis and other N-related metabolites as found from the results that glutamate synthase (GLU1) was upregulated in *W. religiosa*. In contrast, *S. trifasciata* and *W. religiosa* might use serine to generate phosphoglycerate, NADH, and other amino acids and metabolites (Fig. 4). Based on protein expression patterns, the pathway was involved in the interconversion between tetrahydrofolate (THF) and 5-10-methylene-THF. A previous study explained that the major of the one-carbon folate cycle (C_1) was involved in photosynthesis and photorespiration for biosynthetic or regulatory functions (Loizeau et al., 2007). For example, 5-10-methylene-THF is required for the conversion of glycine to serine, thymidylate, and pantothenate synthesis. The methyl group of the compound also is used as a donor for methionine synthesis (Gorelova et al., 2017; Loizeau et al., 2007). Interestingly, all plants except *C. makoyana* are involved in the conversion of glycine to serine or NH_3 through the folate cycle. Therefore, *W. religiosa* was shown, might be the most active in the mechanism, such as the Calvin cycle, pentose phosphate pathway, and photorespiration under PM stress (Fig. 4).

4. Conclusions

In conclusion, the data show the changes in protein profile under PM exposure from cigarette smoke to perform a comparative proteomic analysis of six plant species. Ornamental and perennial plants showed different responses against PM stress. Plants tend to focus on photosynthesis reaction, carbon fixation, and photorespiration mechanisms under PM stress. Most plants are involved in glycine conversion through the folate cycle. Therefore, *W. religiosa* became the most responsive plant in these mechanisms against the PM. This study has identified a set of potential candidates whose identities may help to further understand the intricate regulatory network regulated by the plant in response to PM. The study suggests the network mechanism in the ornamental and perennial plants against PM pollution from cigarette smoke. However, the study needs to confirm in the future. Therefore, the knowledge was necessary to improve plant defense mechanisms and efficiency for phytoremediation against PM stress.

Declarations

Acknowledgment

Authors would like to thank to research funds by National Research Council of Thailand (NRCT), Thailand Science Research and Innovation (TSRI), Program Management Unit for Human Resources & Institutional Development, Research and Innovation, and all those who collaborated to improve the experiment and analysis.

Funding

This research was supported by National Research Council of Thailand (NRCT) project N25A650808, by Thailand Science Research and Innovation (TSRI) Basic Research Fund: The fiscal year 2022 under project number FRB650048/0164, and by the Program Management Unit for Human Resources & Institutional Development, Research and Innovation [grant number B01F630003].

Data availability

The datasets generated during and/or analysed during the current study are available from the corresponding author on reasonable request.

Author contributions

Bayu Hadi Permana wrote the manuscript and analyzed and visualized the data. Phitthaya Nookongbut conducted the experiment and investigation. Sucheewin Krobthong and Yodying Yingchutrakul conducted the analysis and provided technical assistance. Treenut Saithong conducted analysis and visualization. Paitip Thiravetyan conceived the idea and supervision. Chairat Treesubsuntorn conceived the idea and manuscript, and supervision. All the authors discussed and finalized the paper.

Declaration of interests

The authors declare that they have no known competing financial interests or personal relationships that could have appeared to influence the work reported in this paper.

References

1. Cook, D., Fowler, S., Fiehn, O., & Thomashow, M. F. (2004). A prominent role for the CBF cold response pathway in configuring the low-temperature metabolome of Arabidopsis. *Proc Natl Acad Sci U S A*, *101*(42), 15243-15248. https://doi.org/10.1073/pnas.0406069101
2. Foyer, C. H. (2018). Reactive oxygen species, oxidative signaling and the regulation of photosynthesis. *Environmental and Experimental Botany*, *154*, 134-142. https://doi.org/10.1016/j.envexpbot.2018.05.003
3. Gorelova, V., Ambach, L., Rébeillé, F., Stove, C., & Van Der Straeten, D. (2017). Folates in plants: Research advances and progress in crop biofortification. *Front Chem*, *5*, 21. https://doi.org/10.3389/fchem.2017.00021
4. Gupta, R. (2020). The oxygen-evolving complex: A super catalyst for life on earth, in response to abiotic stresses. *Plant Signaling & Behavior*, *15*(12), 1824721. https://doi.org/10.1080/15592324.2020.1824721
5. Henderson, D. P., & Toone, E. J. (1999). Aldolases. In S. D. Barton, K. Nakanishi, & O. Meth-Cohn (Eds.), *Comprehensive Natural Products Chemistry* (pp. 367-440). Pergamon. https://doi.org/10.1016/B978-0-08-091283-7.00088-6

6. Hong, G., Su, X., Xu, K., Liu, B., Wang, G., Li, J., Wang, R., Zhu, M., Li G. (2022). Salt stress downregulates 2-hydroxybutyrylation in Arabidopsis siliques. *Journal of Proteomics*, *250*, 104383.
7. Ifuku, K., Ishihara, S., & Sato, F. (2010). Molecular functions of oxygen-evolving complex family proteins in photosynthetic electron flow. *Journal of Integrative Plant Biology*, *52*(8), 723-734. https://doi.org/10.1111/j.1744-7909.2010.00976.x
8. Jin E.J, Yoon J.H, Bae E.J, Jeong B.R, Yong S.H, Choi M.S. (2021). Particulate matter removal ability of ten evergreen trees planted in korea urban greening. *Forests*, *12*(4):438. https://doi.org/10.3390/f12040438
9. Kim, H., Na, G., Park, S., Ra, S.W., Kang, S.Y., Kim, H.C., Kim, H.C., Lee, S.W. (2021). The impact of life behavior and environment on particulate matter in chronic obstructive pulmonary disease. *Environmental Research*, *198*: 111265.
10. Klein, G., Mathé, C., Biola-Clier, M., Devineau, S., Drouineau, E., Hatem, E., et al. (2016). RNA-binding proteins are a major target of silica nanoparticles in cell extracts. *Nanotoxicology*, *10*, 1555–1564. doi: 10.1080/17435390.2016.1244299
11. Liang, D., Ma, C., Wang, Y. Q., Wang, Y. J., & Chen-Xi, Z. (2016). Quantifying $PM_{2.5}$ capture capability of greening trees based on leaf factors analyzing. *Environmental Science and Pollution Research International*, *23*(21), 21176–21186. https://doi.org/10.1007/s11356-016-7687-9
12. Loizeau, K., Gambonnet, B., Zhang, G.-F., Curien, G., Jabrin, S., Van Der Straeten, D., Lambert, W. E., Rébeillé, F., & Ravanel, S. (2007). Regulation of one-carbon metabolism in Arabidopsis: The N-terminal regulatory domain of cystathionine γ-synthase is cleaved in response to folate starvation. *Plant Physiology*, *145*(2), 491-503. http://www.jstor.org/stable/40065694
13. Nakazato, R.C., Esposito, M.P., Cardoso-Gustavon, P., Buldovas, P., Perdroso, A.N.V., Assis, P.I.L.S., Domingos, M. (2018). Efficiency of biomonitoring methods applying tropical bioindicator plants for assessing the phytotoxicity of the air pollutants in SE, Brazil. *Environ. Sci. Pollut. Res. Int.*, *25*, 19323–19337.
14. Niu L, Zhang H, Wu Z, Wang Y, Liu H, Wu X, et al. (2018) Modified TCA/acetone precipitation of plant proteins for proteomic analysis. *PLoS ONE*, *13*(12): e0202238 10.1371/journal.pone.0202238.
15. Paul, S., Neese, F., & Pantazis, D. A. (2017). Structural models of the biological oxygen-evolving complex: Achievements, insights, and challenges for biomimicry. *Green Chemistry*, *19*(10), 2309-2325. https://doi.org/10.1039/C7GC00425G
16. Paull N.J., Krix D., Irga P.J., Torpy F. R. (2019). Airborne particulate matter accumulation on common green wall plants. *International Journal of Phytoremediation*. 6:1–13. doi:10.1080/15226514.2019.1696744
17. Popek R., Gawrońska H., Gawroński S.W. (2015). The level of particulate matter on foliage depends on the distance from the source of emission. *International Journal of Phytoremediation*. 12: 1262–1268. doi:10.1080/15226514.2014.989312
18. Rai, P. K. (2016). Impacts of particulate matter pollution on plants: Implications for environmental biomonitoring. *Ecotoxicology and Environmental Safety*, *129*, 120-136.

https://doi.org/10.1016/j.ecoenv.2016.03.012

19. Rashid, A., Badhan, A., Deyholos, M., & Kav, N. (2013). Proteomic profiling of the aleurone layer of mature *Arabidopsis thaliana* seed. *Plant Molecular Biology Reporter*, *31*(2), 464-469. https://doi.org/10.1007/s11105-012-0498-3
20. Raudvere, U., Kolberg, L., Kuzmin, I., Arak, T., Adler, P., Peterson, H., Vilo, J. (2019). g:Profiler: a web server for functional enrichment analysis and conversions of gene lists (2019 update). *Nucleic Acids Research*. 47 (W1): W191–W198.
21. Sahu, C., Basti, S., Sahu, S.K. (2021) Particulate Collection Potential of Trees as a Means to Improve the Air Quality in Urban Areas in India. *Environ. Process*. 8, 377–395. https://doi.org/10.1007/s40710-021-00494-3
22. Siswanto, D., Permana, B. H., Treesubsuntorn, C., & Thiravetyan, P. (2020). *Sansevieria trifasciata* and *Chlorophytum comosum* botanical biofilter for cigarette smoke phytoremediation in a pilot-scale experiment—evaluation of multi-pollutant removal efficiency and CO_2 emission. *Air Quality, Atmosphere & Health*, *13*(1), 109-117. https://doi.org/10.1007/s11869-019-00775-9
23. Shen, Z.-J., Qin, Y.-Y., Luo, M.-R., Li, Z., Ma, D.-N., Wang, W.-H., Zheng, H.-L. (2021) Proteome analysis reveals a systematic response of cold-acclimated seedlings of an exotic mangrove plant Sonneratia apetala to chilling stress. *Journal of Proteomics*, *248*, 104349.
24. Sriprapat, W., & Thiravetyan, P. (2016). Efficacy of ornamental plants for benzene removal from contaminated air and water: Effect of plant associated bacteria. *International Biodeterioration & Biodegradation*, *113*, 262-268. https://doi.org/10.1016/j.ibiod.2016.03.001
25. Sriprapat, W., Boraphech, P., & Thiravetyan, P. (2014). Factors affecting xylene-contaminated air removal by the ornamental plant *Zamioculcas zamiifolia*. *Environmental Science and Pollution Research*, *21*(4), 2603-2610. https://doi.org/10.1007/s11356-013-2175-y
26. Swindell, W. R., Huebner, M., & Weber, A. P. (2007). Plastic and adaptive gene expression patterns associated with temperature stress in *Arabidopsis thaliana*. *Heredity*, *99*(2), 143-150. https://doi.org/10.1038/sj.hdy.6800975
27. Tajuelo, M., Rodríguez, D. Rodríguez, A. Escalona, A., Viteri, G., Aranda, A., Diaz-de-Mer, Y. (2020). Secondary organic aerosol formation from the ozonolysis and oh-photooxidation of 2,5-dimethylfuran. *Atmospheric Environment*. *245*: 118041
28. Tiyapairat Y. (2012) Public Sector Responses to Sustainable Haze Management in Upper Northern Thailand. *EnvironmentAsia, 5*(2):1-10. https://doi.org/10.14456/ea.2012.12.
29. Trapp J., Gouveia D., Almunia C., Pible O., Degli E.D., Gaillard J-C., Chaumot A., Geffard O. and Armengaud J. (2018). Digging deeper into the pyriproxyfen-response of the amphipod gammarus fossarum with a next-generation ultra-high-field orbitrap analyser: New perspectives for environmental toxicoproteomics. *Front. Environ. Sci.*, *6*:54. doi: 10.3389/fenvs.2018.00054
30. Treesubsuntorn, C., Setiawan, G. D., Permana, B. H., Citra, Y., Krobthong, S., Yingchutrakul, Y., Siswanto, D., & Thiravetyan, P. (2021). Particulate matter and volatile organic compound

phytoremediation by perennial plants: Affecting factors and plant stress response. *Science of The Total Environment*, *794*, 148779. https://doi.org/10.1016/j.scitotenv.2021.148779

31. Tripathy, B. C., & Oelmüller, R. (2012). Reactive oxygen species generation and signaling in plants. *Plant Signaling & Behavior*, *7*(12), 1621-1633. https://doi.org/10.4161/psb.22455
32. Urrutia-Mosquera, J. A., & Flórez-Calderón, L. Á. (2023). Impact of Confinement on the Reduction of Pollution and Particulate Matter Concentrations. Reflections for Public Transport Policies. *Environ. Process*, 10, 2. https://doi.org/10.1007/s40710-022-00611-w
33. Vizcaíno, J. A., Côté, R. G., Csordas, A., Dianes, J. A., Fabregat, A., Foster, J. M., Griss, J., Alpi, E., Birim, M., Contell, J., O'Kelly, G., Schoenegger, A., Ovelleiro, D., Pérez-Riverol, Y., Reisinger, F., Ríos, D., Wang, R., & Hermjakob, H. (2013). The PRoteomics IDEntifications (PRIDE) database and associated tools: status in 2013. *Nucleic Acids Res*, 41(Database issue), D1063-1069. https://doi.org/10.1093/nar/gks1262
34. Wang D, Zhou B, Fu Q, Zhao Q, Zhang Q, Chen J, Yang X, Duan Y, Li J. 2016. Intense secondary aerosol formation due to strong atmospheric photochemical reactions in summer: observations at a rural site in eastern Yangtze River Delta of China. *Sci Total Environ*. *571*, 1454–1466 (2016).
35. Wang, Y. C. Carbon sequestration and foliar dust retention by woody plants in the greenbelts along two major Taiwan highways. *Ann. Appl. Biol*. *159*, 244–251 (2011).
36. Xiong, H., Hua, L., Reyna-Llorens, I., Shi, Y., Chen, K.-M., Smirnoff, N., Kromdijk, J., & Hibberd Julian, M. (2021). Photosynthesis-independent production of reactive oxygen species in the rice bundle sheath during high light is mediated by NADPH oxidase. *Proceedings of the National Academy of Sciences*, *118*(25), e2022702118. https://doi.org/10.1073/pnas.2022702118

Figures

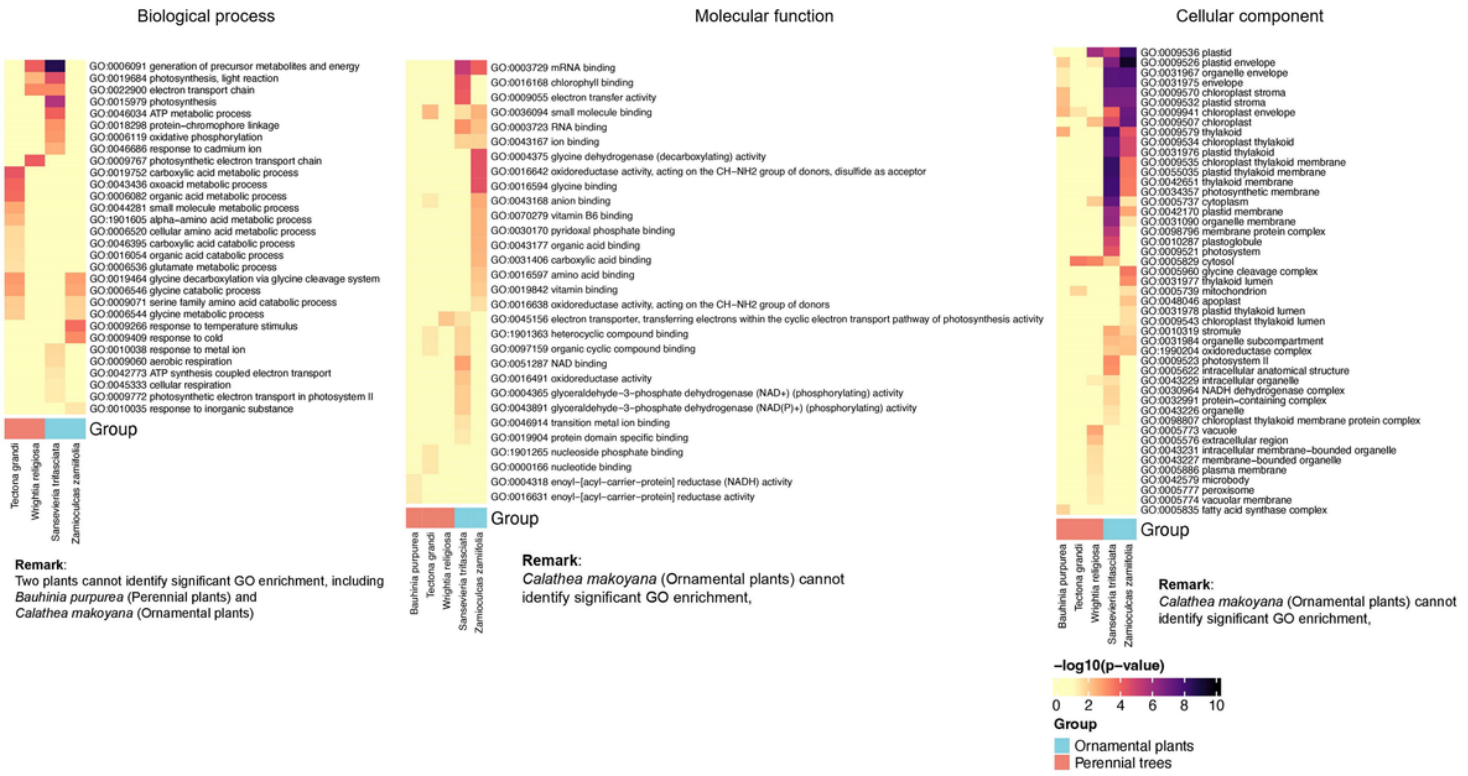

Figure 1

Gene ontology (GO) for biological process, molecular function, and cellular component of ornamental and perennial plants under PM stress from cigarette smoke. Initial PM concentrations were 300-320, 400-450 and 500-530 μg m^{-3} for $PM_{1.0}$, $PM_{2.5}$ and PM_{10}, respectively. *Calathea makoyana* are not able to classify due to not significant GO enrichment.

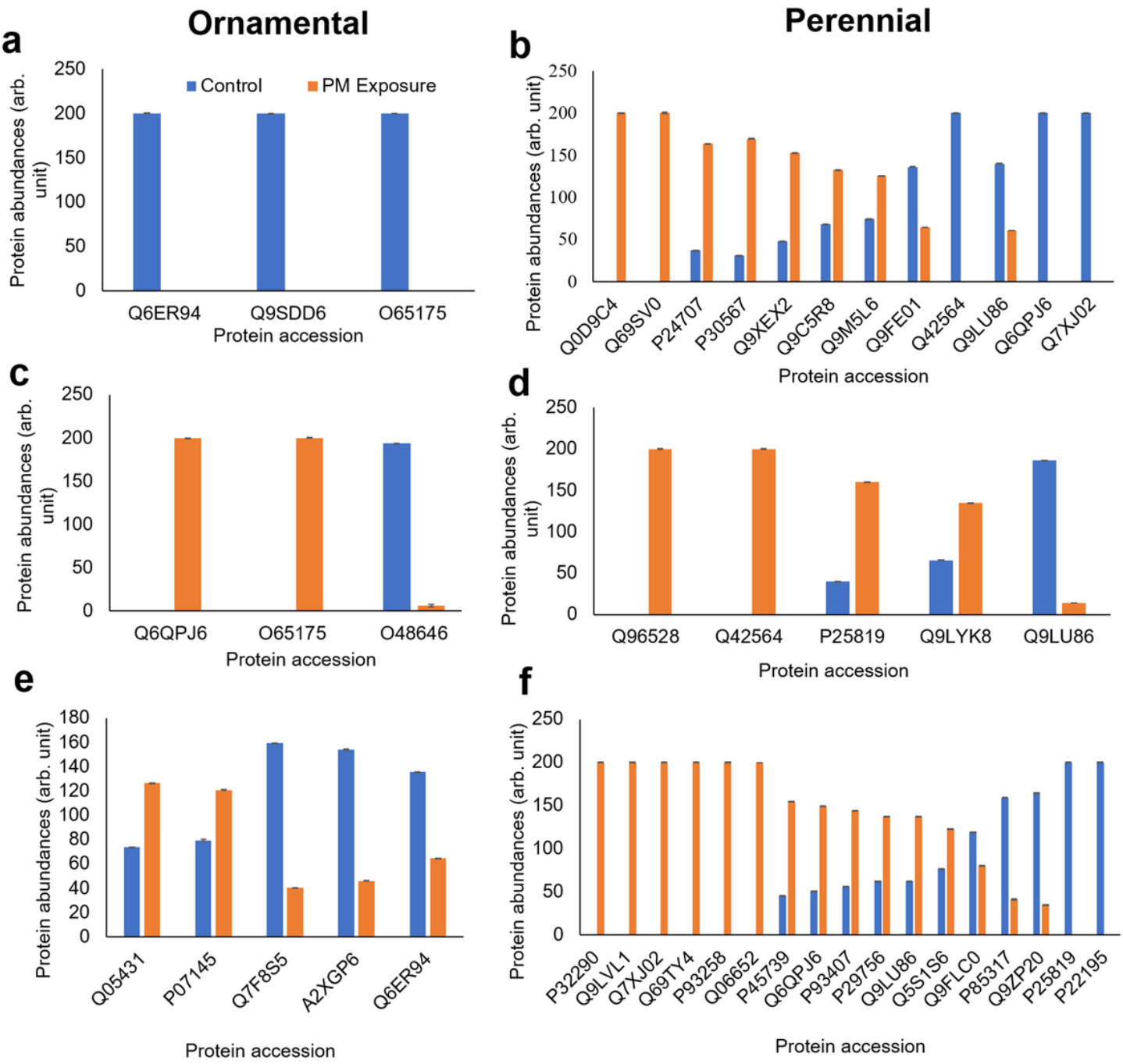

Figure 2

Antioxidants expressed in ornamental and perennial plants under control and PM exposure. (a) *Calathea makoyana*, (b) *Bauhina purpurea*, (c) *Sansevieria trifasciata*, (d) *Tectona grandi*, (e) *Zamioculcas zamiifolia*, (f) *Wrightia religiosa*. The bar graph represents a mean with CV (n=3). Initial PM concentrations were 300-320, 400-450 and 500-530 µg m^{-3} for $PM_{1.0}$, $PM_{2.5}$ and PM_{10}, respectively

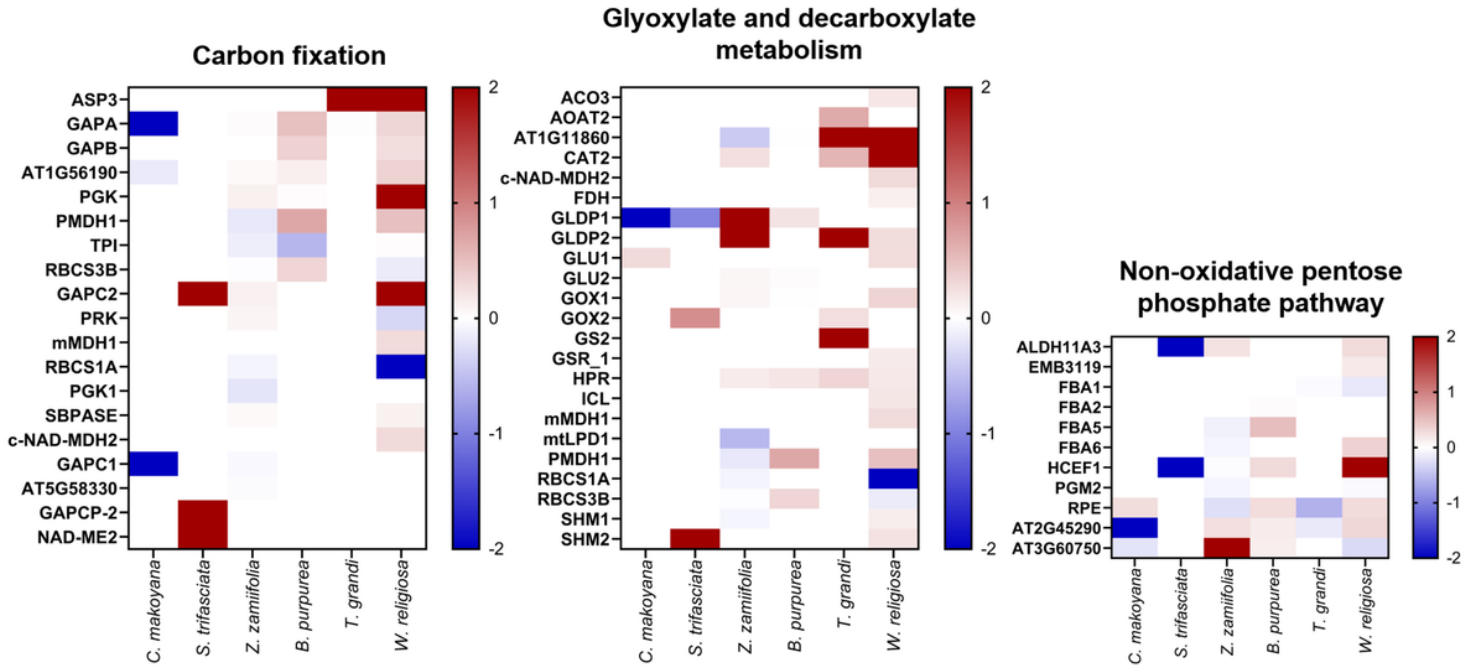

Figure 3

Heatmap of protein expression in ornamental and perennial plants under PM stress. Initial PM concentrations were 300-320, 400-450 and 500-530 μg m^{-3} for $PM_{1.0}$, $PM_{2.5}$ and PM_{10}, respectively. Reddish color represents a more upregulated protein, while the blueish color represents a more downregulated protein.

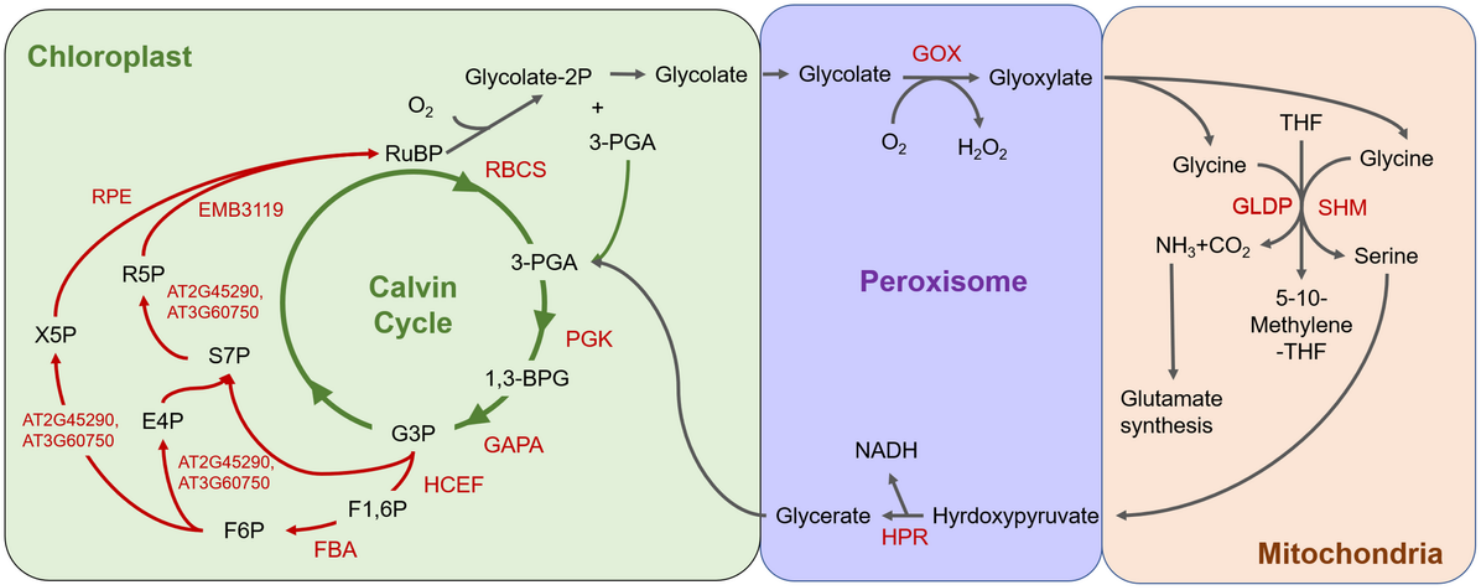

Figure 4

Upregulated proteins related to carbon fixation, pentose phosphate pathway, and photorespiration of *Wrightia religiosa*under PM stress. The red color text represents upregulated proteins, the red arrow is the

pentose phosphate pathway, the green arrow is the Calvin cycle, the gray arrow is the photorespiration pathway, part of folate cycle is in conversion of tetrahydrofolate (THF) to 5-10-methylene THF.